Nested Random Phase Sequence Sets: A Link between AM-FM Demodulation and Increasing Operators with Application to Cardiac Image Analysis

Paul Rodriguez V.[1] and Marios S. Pattichis[1,2]
[1]image and video Processing and Communications Lab (ivPCL)
Department of Electrical and Computer Engineering
The University of New Mexico, Albuquerque, NM 87131-1356
[2]Department of Computer Science
The University of Cyprus, CY-1678 Nicosia, Cyprus
{prodrig, pattichis}@ece.unm.edu

Abstract

AM-FM models images as a linear combination of positive amplitude modulated (AM) sinusoids with non-linear phase functions. In this paper, we develop a novel FM harmonics operator for revealing different levels of image structure detail. The new operator is defined in terms of known AM-FM demodulation techniques: dominant component analysis and channelized component analysis. We also show an example of image segmentation, where the new operator is used for tracking cardiac wall boundaries in Motion-mode (M-mode) ultrasound video.

1 Introduction

Multiscale image analysis has been primarily focused with analyzing images at a number of fixed scales. AM-FM models allow us to consider significant continuous scale variations. In what follows, we motivate and develop a novel FM operator that is capable of extracting different levels of image structure detail.

Consider the Fourier Series expansion of an admissible, one-dimensional, continuous-time signal with period T:

$$f(t) = \sum_{n=-\infty}^{n=\infty} c_n \exp(jn\omega_0 t),$$

where $\omega_0 = 2\pi/T$. Given the phase for the fundamental harmonic $\varphi(t) = \omega_0 t$, we consider the infinite sum

$$s_T(t) = \sum_{n=-\infty}^{n=\infty} \exp[jn\varphi(t)].$$

We know that this infinite sum converges to a constant multiple of the periodic pulse train

$$\sum_{n=-\infty}^{n=\infty} \exp[jn\varphi(t)] = T \sum_{n=-\infty}^{n=\infty} \delta(t - nT).$$

The important property of this final expression is that we can discover the underlying periodic structure of the original signal $f(t)$ from its fundamental component.

Next, we consider two-dimensional images that can be thought off as periodic along some appropriately defined curvilinear coordinate system. This leads to images that have an FM function $\exp(j\varphi(x, y))$ as the fundamental harmonic. We further generalize the model by using a non-negative amplitude function $a(x, y)$ so that the new image model becomes an AM-FM component $a(x, y)\exp(j\varphi(x, y))$. The new model is completely general, capable of describing any image that takes non-zero values. The parameters of the model: (i) the amplitude $a(x, y)$ and (ii) the phase $\varphi(x, y)$ can be estimated using already-developed AM-FM demodulation techniques described in Section 2. We are primarily interested in the phase, since this may reveal the structure of the underlying curvilinear coordinate system.

To recognize how a curvilinear coordinate system might come about, we consider a local model for the level curves of an image: $f(x, y) = c$, for c constant. Locally, we can clearly use the level curves to define a curvilinear coordinate system over which the image remains constant along each level curve, and it changes in the direction orthogonal to the level curves. We can accommodate for the lack of periodicity from period to period using the amplitude function.

Returning to our original expression for periodic signals, we replace t by the coordinate function $\varphi(x, y)$ to get that

0-7803-8387-7/04/$20.00 © 2004 IEEE

the sum of the FM harmonics yields

$$\sum_{n=-\infty}^{n=\infty} \exp\left[jn\omega_0\varphi(x,y)\right] = T \sum_{n=-\infty}^{n=\infty} \delta\left[\varphi(x,y) - nT\right]$$

where T refers the period along the new curvilinear coordinate system.

The previous discussion has served as motivation for our prior work in the use of AM-FM models for image segmentation. Originally, it was restricted to rather specific types of images such as fingerprints, wood-grains, or Motion-mode (M-mode) ultrasound video. In this paper, we want to consider a stochastic model for the phase and suggest applications in a more general setting.

We consider discrete-space finite sums of FM harmonics

$$X_L(n_1,n_2) = \sum_{k=1}^{L} \cos\left[k\varphi(n_1,n_2)\right], \qquad (1)$$

where φ is random with a symmetric, invariant distribution. The basic assumption that the estimated $\varphi(.)$ will have a symmetric distribution was found to hold approximately true for many natural images. However, we do not yet provide general conditions under which this condition will hold. Returning to (1), we observe a very interesting property. Every time we add another FM harmonic, say $\cos\left[L\varphi(n_1,n_2)\right]$, we also add higher frequency components to the previous sum of $L-1$ FM harmonics. Thus, it is clear that the sum images

$$X_1,\ X_2,\ \ldots \qquad (2)$$

progressively add finer and finer details associated with the original image that they are associated with. With the intention of using the new sums for image segmentation, we develop a novel binarization technique that generates binary images based on the sequence of (2). The new method is described in the subsequent Sections. As in mathematical morphology, with some notational abuse, we describe binary images B as the set of pixels (i,j) that satisfy $B(i,j) = 1$, $B = \{(i,\ j) : B(i,j) = 1\}$. Using this new notation, we can show that the generated binary images satisfy a nesting property

$$\ldots \subseteq B_3 \subseteq B_2 \subseteq B_1 \qquad (3)$$

We summarize the entire process by associating operators $\mathcal{T}_i$ that take as input the original input image $f(x,y)$ to generate the binary output images $\mathcal{T}_i\{f\} = B_i$. We note that $\mathcal{T}_L, \mathcal{T}_{L-1}, \ldots, \mathcal{T}_1$ define a sequence of increasing operators in the sense (3).

The binary images reveal important image information regarding image structure. We showed an important application in real-time video tracking of cardiac walls in Motion-mode ultrasound video in [3], and summarize this application in Subsection 4.1. Furthermore, by restricting the phase estimates to come from a particular bandpass filter (Channelized Component Analysis (CCA)), we can extract image contours that are associated with a limited sets of directions.

The rest of the paper is organized as follows. In Section 2, we describe prior work in fast algorithms for AM-FM demodulation. In Section 3, we describe the binarization method in more detail. General application examples are also given in this Section. An application to cardiac image analysis is given in Section 4. Finally, in Section 5, some concluding remarks are given.

2 AM-FM Demodulation

The dominant AM-FM component describes a digital image in terms of:

$$\hat{X}(n_1,n_2) = \sum_{k=1}^{D} \mathrm{I}_{[m(a)=k]} a_k(n_1,n_2) \cos\varphi_k(n_1,n_2) \quad (4)$$

where $\hat{X}(n_1,n_2)$ is the FM harmonic sum of the input image using D different band-pass filters. Note that a channelized AM-FM component can be computed if we consider just one band-pass filter. $\mathrm{I}_{[.]}$ is the indicator function and:

$$a(n_1,n_2) = \max\left\{a_k(n_1,n_2) \ :\ k \in [1,\ D]\right\}$$

$$\mathrm{m}\left(a(n_1,n_2)\right) = \left\{k \ :\ a_k(n_1,n_2) = a(n_1,n_2)\right\}$$

The AM-FM demodulation algorithm operates on the "analytic" version of the original image:

$$X_A(n_1,n_2) = X(n_1,n_2) + j\mathcal{H}\left\{X(n_1,n_2)\right\}$$

where $\mathcal{H}\{.\}$ is the discrete hilbert transformer which operates over the rows or columns of $X(n_1,n_2)$. This is implemented by convolving the rows (or columns) of the original image with an FIR Hilbert transformer; the Kaiser window approximation is used to compute the coefficients of an M^{th} order FIR Hilbert transformer:

$$g_{\mathcal{H}}(n) = (1 - \mathrm{I}_{[n=0]}) \frac{2}{n\pi} \sin^2\left(\frac{n\pi}{2}\right), \quad n \in [-M,\ M]$$

and

$$\mathcal{H}\left\{X(n_1,n_2)\right\} = X(n_1,n_2) * g_{\mathcal{H}}(n_1).$$

Then, for continuous-space signals, the amplitude $a_k(n_1,n_2)$ and phase $\varphi_k(n_1,n_2)$ are estimated from the complex outputs of D bandpass filters using:

$$\hat{X}_{A_k} = X_A * h_k$$

$$\hat{\varphi}_k(n_1,n_2) = \arctan\left[\frac{\mathrm{imag}\left(\hat{X}_{A_k}(n_1,n_2)\right)}{\mathrm{real}\left(\hat{X}_{A_k}(n_1,n_2)\right)}\right]$$

$$\nabla(\hat{\varphi}_k(n_1,n_2)) = \text{real}\left(\frac{\nabla \hat{X}_{A_k}(n_1,n_2)}{j\hat{X}_{A_k}(n_1,n_2)}\right)$$

$$\hat{a}_k(n_1,n_2) = \left|\frac{\hat{X}_{A_k}(n_1,n_2)}{H_k\left(\nabla\hat{\varphi}_k(n_1,n_2)\right)}\right|$$

where $\nabla(\varphi_k(n_1,n_2))$ is the instantaneous frequency and H_k is the frequency response for h_k.

Fast implementation is possible if it is noted that all the operations (with the exception of the arctan) can take advantage of the Single Instruction Multiple Data (SIMD) architecture, which is embedded in most modern microprocessors (i.e: Motorola's PPC 74xx; Intel's PIII, P4, Itanium; AMD's Duron, Athlon, Opterom, etc.). The SIMD architecture has been used to deliver fast implementations of FFTs, convolutions, and AM-FM demodulation [2, 1].

3 AM-FM Binarization and Segmentation

3.1 AM-FM Phase-only reconstruction

We consider AM-FM demodulation using a single bandpass filter. This single channel approach is known as Channelized Component Analysis (CCA). We form the FM harmonic sums for the first L harmonics using:

$$\hat{X}_L = \sum_{k=1}^{L} \cos\left[k\hat{\varphi}(n_1,n_2)\right] \tag{5}$$

We have an interesting property: for symmetric phase distributions, if the $\hat{X}_i$ are normalized between 0 and 1, the FM harmonic sum reconstructed with $L+1$ harmonics is less or equal (pointwise) to the harmonic sum reconstructed with L harmonics. Furthermore, if we threshold all the normalized $\hat{X}_i$ at the same level, we have that the resulting binary images will be nested as given in (3). In this Section, we will give details on the implementation of this statement, outline a proof, and also show applications. Due to lack of space, we cannot give the full proof.

As a consequence of the nesting property, harmonic sum images tend to be darker with the number of added FM harmonics. To illustrate this observation an AM-FM demodulation of the Lena image was carried out, using the CCA algorithm and then reconstructed using (5), followed by binarization. A single, separable, piecewise-linear (in the frequency domain), 5-taps (for the rows and columns) bandpass filter was used. For the columns filter, the bandpass was from $\pi/128$ to $\pi/128+\pi/16$ with transition bands of width $\pi/128$ on either side. For the rows filter, the bandpass was from $-\pi/128$ to $-\pi/128-\pi/16$ with transition bands of width $\pi/128$ on either side. The results in Figure 2 were computed using $1, 5, 10$ and 15 FM harmonics respectively. We note that the white regions continually get thinner and thinner, while they are concentrated around the edges. We also note that more and more detail gets added with the increasing number of harmonics.

3.2 Random Phase Sequences

Let $S = [-\pi,\ \pi)$ and let the random variable $\varphi \in S$ have a symmetric distribution. Let $\hat{X}_L(\varphi)$ be defined as in (5). We have:

$$\hat{X}_L(\varphi) = \sum_{k=1}^{L} \cos\left[k\varphi\right] \tag{6}$$

$$= -0.5 + \frac{\sin(L\varphi+\varphi/2)}{2\sin(\varphi/2)} \tag{7}$$

We note:

$$\hat{X}_{\text{MAX}} = \max_{\varphi\in S} \hat{X}_L(\varphi) = L \tag{8}$$

$$\hat{X}_{\text{MIN}} = \min_{\varphi\in S} \hat{X}_L(\varphi) \tag{9}$$

$$= -0.5 - \frac{1}{2\sin(\frac{3\pi}{4L+2})} \tag{10}$$

We can show that

$$\lim_{L\to\infty} \Pr\left\{\hat{X}_L(\varphi) \le -0.5\right\} = 0.5$$

and then use this fact to show the nesting property (3).

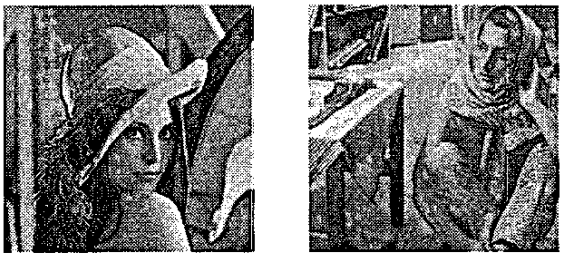

Figure 1. Generic images: Lena and Barbara

As noted earlier, we have observed that our requirement to have a symmetric distribution has been verified empirically using the sample histograms. The sample skewness was also found to be near zero. Empirically, we have observed that the assumption seems to be valid when using between 20 and 50 filter coefficients in the implementation of the FIR Hilbert transformer.

3.3 AM-FM based Binarization

We normalize the FM harmonic image using

$$\hat{X}_L(\varphi) = \frac{\sum_{k=1}^{L} \cos[k\varphi] - \hat{X}_{MIN}}{\hat{X}_{MAX} - \hat{X}_{MIN}}.$$

We then define the binarization scheme using $\hat{B}_L = I_{[\hat{X}_L(\varphi)>\lambda]}$ where $\lambda \in (-\hat{X}_{MIN}/(\hat{X}_{MAX} - \hat{X}_{MIN}),\ 1]$. which eventually leads to $\hat{B}_{L+1} \subseteq \hat{B}_L$.

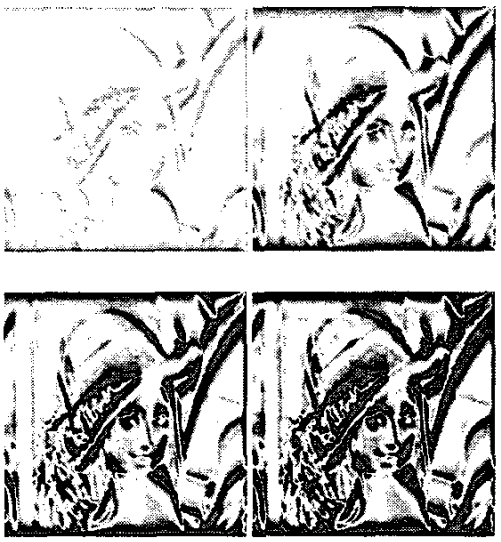

Figure 2. FM harmonic sums using the CCA algorithm when the reconstruction is carried out using (from left to right, top to bottom) 1 , 5 , 10 and 15 harmonics respectively. We note that the more harmonics used in the reconstruction, the darker the image, and the more detail is revealed.

In other words, this scheme leads to a nested set of binary images in which the reconstructed images (and then thresholded) with $L + 1$ harmonics is fully covered by the image reconstructed (and thresholded using the same threshold value) with L harmonics.

3.4 A Second Example

In order to illustrate the usefulness of theory exposed in previous sections, we will use the CCA phase-only algorithm and Barbara's image (Figure 1) as an example. This image shows different objects/patterns: Barbara herself, the table, books in the shelve, patterns in her pants and the tablecloth as well. These objects/patterns have different frequency components. We note that the inclusion property (3) allows us to apply binary morphology to detect a specific object and/or pattern.

We show the FM harmonic sums images for the Barbara image using two different bandpass filters. The first bandpass filter was closer to DC and it is the same one as the one described for the Lena image example. The results from this filter, using 10 FM harmonics refer to the left image in Figure 3. The second bandpass filter was designed the same way, with a row bandpass from $-\pi/4 + \pi/32$ to $-\pi/4 - \pi/32$, a column bandpass from $\pi/4 - \pi/32$ to $\pi/4 + \pi/32$, and transition band widths of $\pi/128$. The results from this filter, using 5 FM harmonics refer to the right image in Figure 3. For the left image, we can see edges from big objects being emphasized. For the right image, we see edges associated with high-frequencies contained in the bandpass of the second filter. We extend the idea of using different bandpass filters to emphasize different regions in the next Section.

Figure 3. FM harmonic sums results.

4 Application to Cardiac Image Analysis

4.1 Preliminary results for M-mode Echocardiography

Based on the previous results, we propose a method to automatically segment cardiac walls present in M-mode echocardiography images without any manual interaction from the users. The cardiac walls include the anterior right ventricular wall, the interventricular septum walls and the left ventricular posterior wall. Using the segmented walls, five clinical measurements (see [4]) can be made for the assessment of heart function as shown in Figure 4: Right ventricular dimension at end-systole (RVDD), septal thickness at end-diastole (Sept), left ventricular dimension at end-systole (LVSD), left ventricular dimension at end-diastole (LVDD) and the left ventricular posterior wall thickness measure at end-diastole (LVPW).

The segmentation of the M-mode echocardiogram is implemented in three consecutive steps, which are summarized as follows (a more complete description can be found in [3]).

For step 1, a very low-frequency (in both directions) bandpass filter is used so as to get a coarse approximation of regions of interest (see Section 3). In step 2, high-frequency filtering in the vertical direction is used for extracting the

wall boundaries. In both steps 1 and 2, an FM reconstruction of the original image is computed using multiple harmonics (6).

The reconstructed image is binarized using the ideas described in Subsection 3.3. The resulting image is then used to compute the regions of interest (ROI) in the input image (see [2]). The output of step 2 is a set of curves and a small ROI around each curve, which defines the boundaries of the interventricular septum and the left posterior ventricular wall. Due to the sinusoidal shape of the walls present in M-mode echocardiography, this curve is restricted to be a linear combination of E cosine functions, where E depends on energy constrains. A local search is performed which minimizes the curve energy, as well as the potential energy of the input image, is performed to find an accurate estimate of the walls' boundaries; this is an energy minimization formulation of a deformable open contour. If after the local search, the resulting curve (boundary) does not meet a smoothness condition it is dropped and the boundary is marked as missed.

The dataset used in the present work were two M-mode echocardiography videos (10 seconds each). The videos were acquired using a Matrox framegrabber connected to the analog video output of the Acuson (Sequoia, Acuson C256, Mountain View, CA 94043). In each case, the frequencies of the ultrasound probes were: 6.5 MHz and 4.0 MHz.

A result of applying the proposed method is shown in Figure 5. In this case the algorithm is able to find well-defined boundaries for the left ventricular wall and between blood-pool and the Septum. It must be noted that measurements such as LVPW, LVSD and LVDD can be easily made from the segmented walls. The input image is a frame taken from a 10 seconds M-mode video (ultrasound device was set to use 6.5 Mhz.)

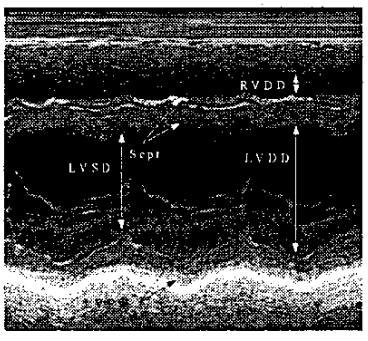

Figure 4. M-mode echocardiogram showing desired measurements.

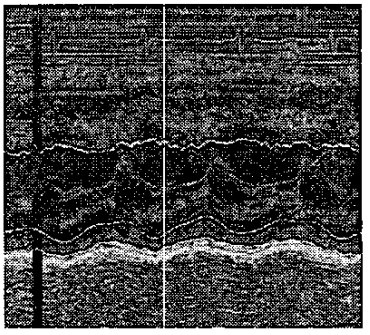

Figure 5. Proposed method's result (6.5 Mhz). All three walls are correctly tracked: the ventricular posterior walls and the interventricular septum wall.

5 Conclusion

We presented a new FM operator defined in terms of an image phase estimate. We show that the new operator can reveal image structure at an increasing level of detail, while it generates a nested sequence of binary images. An application to cardiac wall tracking in Motion-mode ultrasound video is discussed, where it is shown that difficult wall boundaries can be estimated with the new operator.

References

[1] P. Rodríguez. Fast am-fm demodulation with applications to real-time image and motion mode video analysis. Ph.D. proposal, The University of New Mexico, 2003.

[2] P. Rodríguez, R. Jordan, M. Pattichis, and M. B. Goens. Fast am-fm demodulation image and video analysis using single instruction multiple data (simd) architectures. In *International Conference on Signal Processing, Pattern Recognition and Applications*, Rhodes, Greece, June 2003.

[3] P. Rodríguez, M. Pattichis, and M. B. Goens. M-mode echocardiography image and video segmentation based on am-fm demodulation techniques. In *International Conference of the IEEE Engineering in Medicine and Biology Society*, Cancun, Mexico, September 2003.

[4] A. R. Snider, G. A. Serwer, and S. B. Ritter. *Echocardiography in Pediatric Heart Disease*. Mosby-Yera Book, Inc, second edition, 1997.